RSC Advances

This article can be cited before page numbers have been issued, to do this please use: A. Srivastava, A. Agarwal, S. K. Gupta and N. Jain, *RSC Adv.*, 2016, DOI: 10.1039/C6RA02458K.

ROYAL SOCIETY OF CHEMISTRY

www.rsc.org/advances

View Article Online
DOI: 10.1039/C6RA02458K

Journal Name

COMMUNICATION

Graphene oxide decorated with Cu(I)Br nanoparticles: A reusable catalyst for the synthesis of potent bis(indolyl)methane based anti HIV drugs

Received 00th January 20xx,
Accepted 00th January 20xx

DOI: 10.1039/x0xx00000x

www.rsc.org/

Ananya Srivastava,[a] Aakanksha Agarwal,[b] Satish K Gupta,[b] and Nidhi Jain*[a]

A GO-Cu(I)Br nanocatalyst has been prepared, and applied for the synthesis of bis(indolyl)methanes. The catalyst is highly effective, is required in much lower amount (0.05 mol%), and is recyclable up to six reaction cycles without loss in activity. The synthesized compounds have been screened for their *in vitro* anti-HIV activity, and compound 3d has shown significant anti-HIV-1 effect. Molecular modelling of 3d with reverse transcriptase enzyme has been carried out to understand its binding mechanism to the active enzyme site.

Bis(indolyl)methanes (BIMs) are biologically significant molecules, and are found in many plant and marine sources.[1] They are known to possess various therapeutic effects such as antimicrobial,[2] antifungal,[3] antiandrogenic,[4] growth promoting,[5] and anticancer activities.[6,7] Synthetic BIMs have been used not only for biological applications but also as dyes, and colorimetric sensors.[8] Due to the potent biological profile of BIMs, continuous efforts have been dedicated towards the development of efficient strategies for their synthesis. Most of the synthetic routes employ homogenous catalysis involving electrophilic substitution reaction of indole with carbonyl compounds. A variety of protic and Lewis acid catalysts have been reported for mediating this synthesis.[9] Although homogeneous catalysis is quite advantageous in terms of product yield and efficiency, it suffers from limitations of catalyst recovery and problem of residual catalyst in the synthesized molecules.[10] Therefore, extension of these methods for large-scale synthesis becomes a matter of environmental and economic concern. The use of supported catalysts offers an attractive solution owing to their easy separation, convenient handling, non-toxic nature, and ability to be reused.[11] Some of the solid supported catalytic systems used for the synthesis of BIMs include amberlyst-15,[12] cellulose, poly (ethylene glycol)[13] and silica.[14] In recent years graphene oxide (GO) has been recognized as an attractive support for heterogeneous nanocatalysis owing to its unique physical and chemical properties such as large surface area, good chemical stability, high absorption coefficient, and excellent conductivity.[15] It has a two-dimensional sp2 - hybridized carbon structure functionalized with epoxide, hydroxyl and carboxyl groups. GO supported catalysts have been developed for cross-coupling reactions,[16] oxygen reduction reaction,[17] epoxidation of alkenes,[18] reduction of nitrophenol,[19] click reaction[20] etc. In our efforts directed towards developing efficient catalysis using copper and palladium, we prepared a novel nanocatalytic system comprising of graphene oxide supported Cu(I)Br. The catalyst was tested for its efficacy by employing it for the synthesis of bis(indolyl)methane derivatives. Further, the synthesized 3-3' linked BIMs were screened for their anti HIV activity.

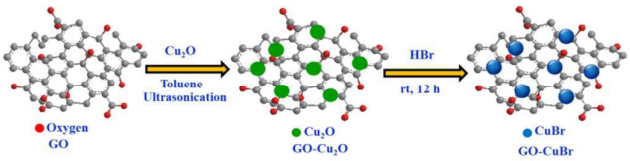

Scheme 1. Schematic representation of the synthesis of GO-CuBr nanocatalytic system.

A modified Hummer's method was used to synthesize GO from graphite, the details are given in ESI†.[21] GO supported CuBr nanocatalyst was prepared using cuprous oxide, followed by treatment with HBr in glacial acetic acid (Scheme 1). The catalyst was isolated and characterised for the presence of various chemical functionalities by PXRD, FTIR, and RAMAN spectroscopy (Fig. 1). Fig. 1a shows the comparative PXRD patterns for graphite, graphene oxide and GO–CuBr nanocomposite. The original graphite powder showed a sharp characteristic diffraction peak at 2θ=26.5°, corresponding to the (002) crystal plane. After the oxidative treatment of graphite, the (002) diffraction peak shifted to lower angle at 2θ=10.5° corresponding to (001) plane, indicating the formation of graphene oxide. Complete disappearance of graphite peak confirmed the successful total conversion of

[a]*Department of Chemistry, Indian Institute of Technology, New Delhi-110016; *E-mail: njain@chemistry.iitd.ac.in; Fax: +91 11 26581102; Tel: +91 11 26591562.*[b]*National Institute of Immunology, New Delhi-110067;* †Electronic Supplementary Information (ESI) available: Detailed experimental procedures, copies of ^{1}H NMR and ^{13}C NMR. See DOI: 10.1039/x0xx00000x

View Article Online
DOI: 10.1039/C6RA02458K

graphite to graphene oxide. The GO–CuBr composite showed four characteristic diffraction peaks of CuBr at 27.2, 45.1, 53.4, and 65.6 corresponding to (111), (220), (311) and (400) planes respectively (face centered cubic, JCPDS card no. 77-1997). The peak of GO was not observed in the XRD of GO–CuBr nanocomposite since the regular stack of GO was destroyed by intercalation of CuBr NPs.

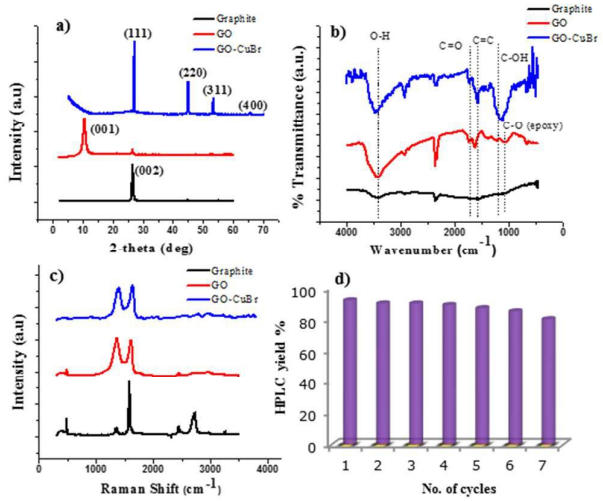

Fig. 1 a) PXRD, b) FTIR, c) RAMAN spectra of graphite, GO, and GO-CuBr, d) recycling of GO-CuBr as catalyst.

Fig. 1b compares the FTIR patterns of graphite, GO and GO–CuBr. The oxidation of graphite powder leads to introduction of various functional groups, the nature of which could be determined by FTIR. Appearance of an intense and broad peak at 3419 cm^{-1} was attributed to the stretching mode of O–H bond, and revealed the abundance of hydroxyl groups in GO. A strong absorption band at 1727 cm^{-1} (C=O) represented carboxylic acid and carbonyl groups while the characteristic band of C=C appeared at 1627 cm^{-1}. Furthermore, the bands at 1222 cm^{-1} and 1064 cm^{-1} indicated the presence of C–OH and C–O (epoxy) groups, respectively in GO. All these peaks confirmed the successful transformation of graphite into GO. On incorporating CuBr to GO, two major differences were observed in the spectra. The first was the decrease in intensity of carbonyl peak at 1727 cm^{-1} and the second was the appearance of an intense peak at 1143 cm^{-1} corresponding to the C–O bond. Both these changes suggested the bonding of copper to carbonyl group of GO and introduction of partial single bond character in it.

As depicted by Raman (Fig. 1c), D band at 1350 cm^{-1} and G band at 1580 cm^{-1} corresponding to typical features of GO was observed. In the next step, the reduction in the intensity of D band, complimented with an enhancement in the G band intensity suggested the prevalent metal–carbon interactions in GO–CuBr.

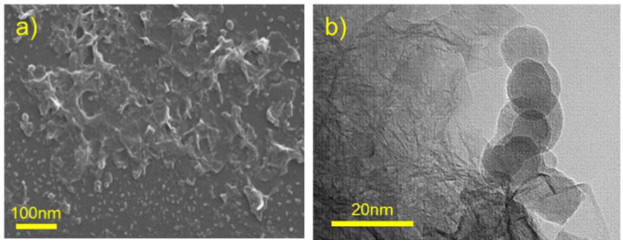

Fig. 2 a) SEM and b) TEM images of GO-CuBr nanocatalytic system.

The morphological and structural features of the nanocomposite were determined by SEM and TEM analysis (Fig. 2). A uniform distribution of CuBr NPs on the surface of the GO nanosheets with an average particle size of around 10 nm was observed. The energy dispersive X-ray (EDX) spectroscopy further confirmed the presence of copper and bromine on GO surface (Fig. S1).

Table 1 Synthesis of BIMs using GO-CuBr nanocatalyst.[a]

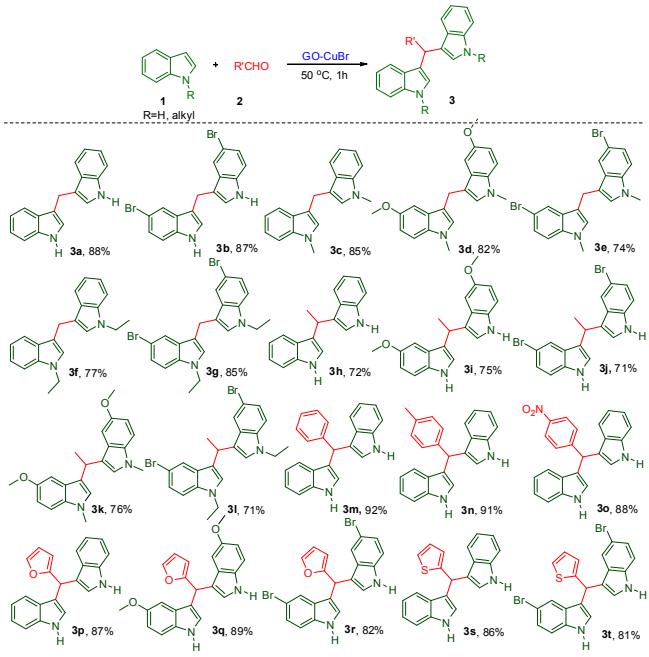

[a]Reaction conditions: Isolated yield, **1** (2.0 equiv., 1.88 mmol), **2** (1.0 equiv., 0.94 mmol), GO-CuBr (0.05 mol%) at 50 °C for 1 h.

The catalytic potential of the prepared GO–CuBr nanocatalyst was determined by using it for the synthesis of bis(indolyl)methanes, as shown in Table 1. A model reaction between benzaldehyde (1 equiv.), and indole (2 equiv.) in the presence of 5 mol% GO–CuBr at 50 °C yielded 3,3'-(phenylmethylene) bis(1H-indole) **3m** as the sole product in 92% yield under solvent-free conditions. We were delighted to see that reducing the catalyst loading to 2 mol%, 1 mol%, 0.5 mol% and 0.05 mol% did not affect the product yield, demonstrating the efficacy of the nanocatalyst in mediating the electrophilic substitution reaction of indole with aldehyde. However, further reduction in the amount of catalyst to 0.025

View Article Online
DOI: 10.1039/C6RA02458K

mol% decreased the yield to 77%, while no product was observed in the absence of the catalyst. To explore the generality of the reaction, various indoles and aldehydes were chosen as substrates. It was found that with *N*-substituted as well as unsubstituted indoles, high yield of BIMs was obtained. Similarly, both methoxy and bromo substituents on the indole ring gave high yield of the corresponding BIM derivatives. Bromo group was found to be intact in the product, thus providing a handle for further derivatisation of the molecule (**3b, 3e, 3g, 3j, 3l, 3r** and **3t**). Various aliphatic (**3a-3l**) and aromatic (**3m-3t**) aldehydes were screened, and were found to exhibit a similar reactivity towards indole. Electron donating methyl substituent (**3n**) as well as electron withdrawing nitro substituent (**3o**) on the aldehyde well-tolerated the reaction conditions, and similar yield of the corresponding products was obtained. The substrate scope was further extended to heterocyclic aldehydes. It was found that the reaction went well with 2-furan and 2-thiophene aldehydes, and the corresponding heteroaryl substituted BIMs (**3p-3t)** were obtained in high yields.

Table 2 *In vitro* cytotoxicity and anti HIV-1 activity of the synthesized compounds using TZM-bl cells based assay[a]

S. No.	Sample Code	TZM-bl cells (μM)		TI[c]
		CC_{50}[a]	IC_{50}[b]	
1	3a	71.9 ± 0.4	NS	-
2	3b	30.5 ± 14.3	22.4 ± 8.0	1.35
3	3c	127.4 ± 0.1	55.6	2.29
4	**3d**	**67.6 ± 0.4**	**0.7 ± 0.03**	**95.04**
5	3e	8.4 ± 0.2	NS	-
6	3f	85.3 ± 1.1	44.2 ± 0.03	1.93
7	3g	135.5 ± 8.1	NS	-
8	3h	38.1 ± 0.1	41.0 ± 2.9	0.92
9	3i	65.0 ± 1.1	34.9 ± 6.6	1.86
10	3j	30.6 ± 0.7	67.5 ± 9.1	0.45
11	3k	40.5 ± 0.5	NS	-
12	3l	35.8 ± 0.3	44.3 ± 6.4	0.81
13	3m	48.7 ± 1.5	NS	-
14	3n	43.1 ± 1.7	NS	-
15	3o	46.0 ± 1.2	44.4 ± 5.5	1.03
16	3p	56.4 ± 0.7	NS	-
17	3q	60.9 ± 0.8	NS	-
18	3r	45.5 ± 0.4	NS	-
19	3s	92.6 ± 1.4	31.4 ± 2.4	2.95
20	3t	34.9 ± 0.6	NS	-

[a]CC_{50}: The cytotoxic concentration of the compound that caused the reduction of viable cells by 50%. [b]IC_{50}: The concentration of the compound that resulted in 50% inhibition of HIV-1 infection. All data presented are average of 3 independent experiments performed in duplicates. [c]TI: Therapeutic index, it is CC_{50} /IC_{50}. NS: Not significant.

Next, the reusability of the catalyst was determined. After completion of the reaction, dichloromethane was added to the reaction mixture to dissolve the product. The insoluble catalyst was separated from the reaction mixture by centrifugation, washed with dichloromethane, and dried at 50 °C in the oven. The recovered catalyst was used for the next batch of reaction, and was found to be potentially active up to six cycles (Fig. 1d). In the seventh recycle though, product **3m** was obtained with a 13% reduction in yield.

Human immunodeficiency virus (HIV) is a lentivirus that causes one of the most challenging diseases of the current time, acquired immunodeficiency syndrome (AIDS). According to a report of the Joint United Nations Program on HIV/AIDS, approximate 34 million people in the world are living with HIV with no promising treatment. Therefore, the development of effective, safe, and affordable anti-HIV drugs is highly desirable. There are only a few literature reports that reveal bisindole nucleus to possess anti-HIV properties.[22] This inspired us to synthesize bisindole derivatives, and evaluate the anti-HIV activity of the synthesized library of 3-3' linked BIMs.

The inhibitory activity of the compounds is sometimes a result of their toxic effects, and therefore might resemble an inaccurate conclusion. Prior to the analysis of anti-HIV activity, compounds **3a-3t** were tested *in vitro* for their cytotoxicity using MTT assay[23] and the results are summarized in Table 2. The CC_{50} value indicates the cytotoxic concentration of the compound leading to 50% reduction in cell viability. Out of the 20 compounds evaluated by MTT assay, five compounds **3g**, **3c**, **3s**, **3f** and **3a** showed CC_{50} values of more than 70 μM. Subsequently, we examined the *in vitro* inhibition of HIV-1 infection by reporter-gene based cell assay system using TZM-bl cells for the compounds (**3a-3t**), and calculated IC_{50} values as described previously[24] (Table 2). While all compounds showed a positive anti-HIV-1 effect, the maximum activity was exhibited by **3d.** It showed the IC_{50} value of 0.712 ± 0.035 μM, which is considerably significant compared to IC_{50} values of other compounds ranging between 22.46 to 67.51 μM. In the final *in vitro* drug efficacy analysis, we evaluated the therapeutic index (TI) of these compounds, which is a measure of the amount of drug that causes the therapeutic effect to the amount that causes toxicity. The TI value for **3d** was the highest (95.04) among all the synthesized molecules, clearly distinguishing it to be a potent anti-HIV-1 molecule. Overall, these studies reveal that the synthesized library can inhibit HIV-1 infection, and may be a useful lead for the design and development of new anti-HIV drugs.

To rationalize the results of the *in-vitro* biological assays and understand the binding ability of these molecules with reverse transcriptase enzyme, we decided to perform a molecular modelling analysis of compounds **3a–3t**. The docking analysis was carried out using the Swissdock webserver (The Molecular Graphics Laboratory, Scripps Research Institute). Swissdock binding energy scores ranging from −8.32 to −7.09 kcal mol^{-1} were obtained for all the compounds, which is very close to the control nevirapine (-8.62 kcal mol^{-1}), suggesting that the tested compounds might be functioning by inhibiting the enzyme. According to the inhibition results and binding energy, **3d** was selected as a typical ligand. The 2D and 3D pictures of **3d** and nevirapine binding with reverse transcriptase enzyme are illustrated in Fig. 3.

View Article Online
DOI: 10.1039/C6RA02458K

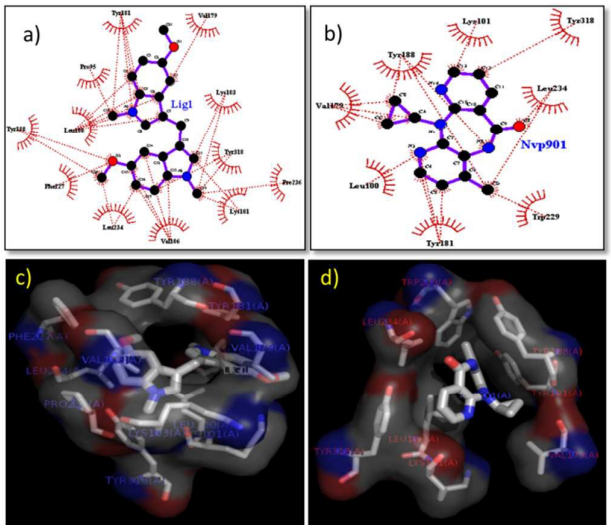

Fig. 3 2D model for binding mode of a) **3d** and b) nevirapine into the binding site of reverse transcriptase enzyme; 3D model for binding mode of c) **3d** and d) nevirapine into the binding site of reverse transcriptase enzyme.

For compound **3d,** the amino acids Pro95, Leu100, Lys101, Lys103, Val106, Val179, Tyr181, Tyr188, Phe227, Leu234, Pro236 and Tyr318 are showing hydrophobic interactions (Fig. 2a) which are very similar to the nevirapine interactions.[25] The amino acid residues composing the non-nucleoside binding site for nevirapine are mainly hydrophobic. Figure 3b shows the binding site of RT complexed to the control NNRTI nevirapine. Furthermore, it is clearly evident from the 3D model that compound **3d** interacts with the same binding pocket of the reverse transcriptase enzyme where nevirapine also binds. The docking analysis showed that the orientations of the lead compound nevirapine, and **3d** are similar in the binding pocket of reverse transcriptase enzyme (Fig. 3c and 3d). Thus, the binding energy and hydrophobic interactions with amino acids in active site of the target enzyme are in good agreement with the observed anti HIV-1 activity of **3d**.

Conclusions

In summary, we have prepared GO-CuBr nanocomposite, and demonstrated it as a highly efficient catalyst for the synthesis of BIMs. The catalyst is required in very low amount, gives high yield of products, and is recyclable. Furthermore, compound **3d** has been established as a potent anti HIV-1 drug *via* TZM-bl cells based assay and molecular modelling analysis.

This work has been financially supported by the Department of Science and Technology, India (SR/FT/CS-08/2011), Department of Biotechnology, India (BT/PR5691/MED/108/11/2012), and Indian Council of Medical Research (5/7/853/12-RCH). A.S. thanks Council of Scientific and Industrial Research, India for graduate fellowship. The authors thank DST-FIST for funding the ESI-HRMS facility at IIT Delhi.

Notes and references

1 a) U. Pindur and T. Lemster, *Current Medicinal Chemistry*, 2001, **8**, 1681–1698. b) A. J. Kochanowska-Karamyan and M. T. Hamann, *Chem. Rev.*, 2010, **110**, 4489–4497.
2 G. Sivaprasad, P. T. Perumal, V. R. Prabavathy and N. Mathivanan, *Bioorg. Med. Chem. Lett.*, 2006, **16**, 6302–6305.
3 S. Sakemi and H. H. Sun, *J. Org. Chem.*, 1991, **56**, 4304–4307.
4 H. T. Le, C. M. Schaldach, G. L. Firestone and L. F. Bjeldanes, *J. Biol. Chem.*, 2003, **278**, 21136–21145.
5 C. Pal, S. Dey, S. K. Mahato, J. Vinayagam, P. K. Pradhan, V. S. Giri, P. Jaisankar, T. Hossain, S. Baruri, D. Raya and S. M. Biswas, *Bioorg. Med. Chem. Lett.* 2007, **17**, 4924-4928.
6 A. McDougal, M.S. Gupta, D. Morrow, K. Ramamoorthy, J.E. Lee, and S.H. Safe, *Breast Cancer Res Treat*, 2001, **66**, 147-157.
7 S. Safe, S. Papineni and S. Chintharlapalli, *Cancer Letters*, 2008, **269**, 326-338.
8 a) T. J. Novak, D. N. Kramer, H. Klapper, L. W. Daasch, B. L. Murr, *J. Org. Chem.* 1976, **41**, 870. b) X. He, S. Hu, K. Liu, Y. Guo, J. Xu and S. Shao, *Org. Lett.*, 2006, **8**, 333–336.
9 M. Shiri, M. A. Zolfigol, H. G. Kruger and Z. Tanbakouchian, *Chem. Rev.*, 2010, **110**, 2250–2293.
10 a) P. T. Anastas and J. C. Warner ed. ''Green Chemistry Theory and Practice'', Oxford University Press, Oxford, 1998. b) P. T. Anastas and T. C. Williamson, ed. Green Chemistry Frontier in Benign Chemical Synthesis and Processes, Oxford Univ. Press, Oxford, 1998. c) C. Christ, Ed. ''Production Integrated Environmental Protection and waste Managements in the Chemical Industry, Wiley–VCH, Weinheim, 1999.
11 a) M. J. Climent, A. Corma and S. Iborra, *Chem. Rev.*, 2011, **111**, 1072–1133. b) A. Corma and H. García, *Chem. Rev.*, 2002, **102**, 3837–3892. c) Q.-H. Fan, Y.-M. Li and A. S. C. Chan, *Chem. Rev.*, 2002, **102**, 3385–3466.
12 C. Ramesh, J. Banerjee, R. Pal and B. Das, *Adv. Synth. Catal.,* 2003, **345**, 557-559.
13 S. -R. Sheng, Q. -Y. Wang, Y. Ding, X. -L. Liu, M. -Z. Cai, *Catal Lett.*, 2009, **128**, 418–422.
14 K. Reddi Mohan Naidu, B. Satheesh Krishna, M. Anil Kumar, P. Arulselvan, S. Ibrahim Khalivulla and O. Lasekan, *Molecules*, 2012, **17**, 7543–7555.
15 a) Y. Liu, X. Dong and P. Chen, *Chem. Soc. Rev.*, 2012, **41**, 2283–2307. b) B. F. Machadoab and P. Serp, *Catal. Sci. Technol.*, 2012, **2**, 54.
16 D. Liua, C. Zhanga, F. Wanga, Z. Huanga, N. S. Zhanga, H. Zhou and Y. Kuang, *J. Mater. Chem. A*, 2015, **3**, 16583-16589.
17 M. Sun, H. Liu, Y. Liu, J. Qu and J. Li, *Nanoscale*, 2015, **7**, 1250–1269.
18 M. Liu, X. Wang, Y. Chen and L. Dai, *RSC Adv.,* 2015, **5**, 61481-61485.
19 J. Luo, N. Zhang, R. Liu and X. Liu, *RSC Adv.*, 2014, **4**, 64816-64824.
20 X. Xiong, H. Chen, Z. Tang and Y. Jiang, *RSC Adv.*, 2014, **4**, 9830-9837.
21 W. S. Hummers and R. E. Offeman, *J. Am. Chem. Soc.*, 1958, **80**, 1339–1339. b) J. Liu, H. Jeong, J. Liu, K. Lee, J.-Y. Park, Y. H. Ahn and S. Lee, *Carbon*, 2010, **48**, 2282–2289.
22 M.-Z. Zhang, Q. Chen and G.-Fu Yang, *Eur. J. Med. Chem.*, 2015, **89,** 421-441.
23 T. Mossman, *J. Immun. Methods*, 1983, **65**, 55-63.
24 Nutan, M. Modi, C. S. Dezutti, S. Kulshreshtha, A. K. S. Rawat, S. K. Srivastava, A. Verma, U. Ranga, S. Malhotra and S. K. Gupta, *Virology Journal*, 2013, **10**, 309.
25 Z. Zhou, M. Madrid and J. D. Madura, *Proteins*, 2002, **49**, 529–542.

View Article Online
DOI: 10.1039/C6RA02458K

Graphical abstract

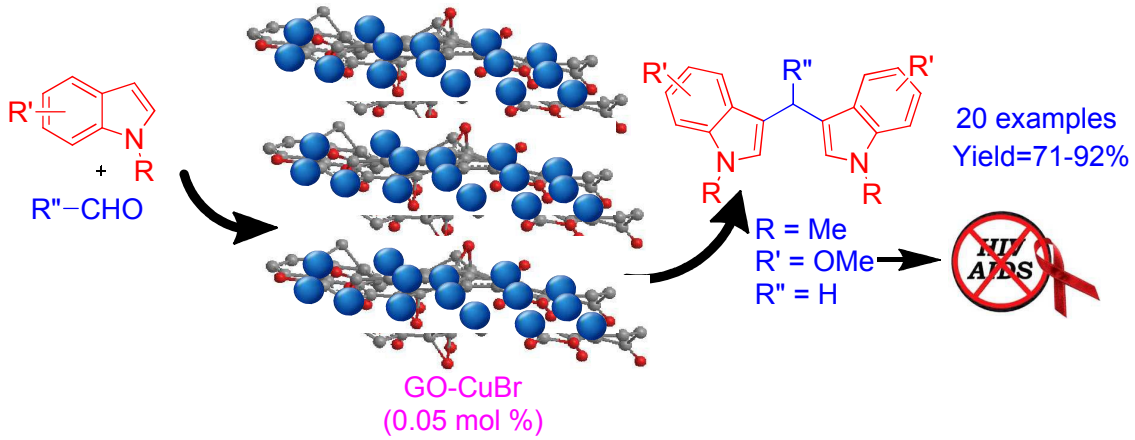

A reusable nanocatalytic system comprising of Cu(I)Br decorated on graphene oxide has been prepared and applied for an efficient synthesis of bis(indolyl)methanes, bringing down the catalyst requirement to 0.05 mol% only. The synthesized compound **3d** shows significant anti-HIV activity. Molecular modeling of **3d** with reverse transcriptase enzyme has been carried out to understand its binding mechanism to the active enzyme site.